Journal of Colloid and Interface Science 631 (2023) 260–271

Contents lists available at ScienceDirect

Journal of Colloid and Interface Science

journal homepage: www.elsevier.com/locate/jcis

Effect of surfactants on the thermoresponse of PNIPAM investigated in the brush geometry

Isaac J. Gresham [a,1], Joshua D. Willott [b,c], Edwin C. Johnson [c,2], Peixun Li [d], Grant B. Webber [c], Erica J. Wanless [c], Andrew R.J. Nelson [e], Stuart W. Prescott [a,*]

[a] School of Chemical Engineering, UNSW Sydney, Science and Engineering Building Gate 2, High Street, UNSW, 2052 NSW, Australia
[b] Membrane Science and Technology, Mesa+ Institute for Nanotechnology, University of Twente, Enschede, 7500 AE, the Netherlands
[c] ARC Centre of Excellence for Enabling Eco-Efficient Beneficiation of Minerals, University of Newcastle, Callaghan, 2308 NSW, Australia
[d] ISIS Facility, Rutherford Appleton Laboratory, STFC, Chilton, Didcot OX11 0QX, UK
[e] ANSTO, Locked Bag 2001, Kirrawee DC, 2232 NSW, Australia

GRAPHICAL ABSTRACT

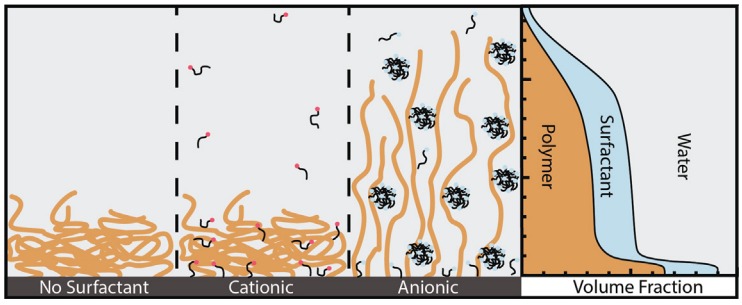

ARTICLE INFO

Article history:
Received 4 August 2022
Revised 10 October 2022
Accepted 15 October 2022
Available online 25 October 2022

Keywords:
poly(*N*-isopropylacrylamide)
Polymer brushes
Sodium dodecylsulfate
Surfactants
Responsive polymers

ABSTRACT

Hypothesis: Anionic surfactants have been reported to interact with poly(*N*-isopropyl acrylamide) (PNIPAM), suppressing its thermoresponse. Scattering and NMR studies of the anionic sodium dodecylsulfate (SDS) system propose that the PNIPAM-surfactant interaction is purely hydrophobic. However, prior phenomenological investigations of a range of surfactant identities (anionic, cationic, nonionic) show that only anionic surfactants affect the thermoresponse and conformation of PNIPAM, implying that the hydrophilic head–group also contributes. Crucially, the phenomenological experiments do not measure the affinity of the tested surfactants to the polymer, only their effect on its behaviour.
Experiments: We study the adsorption of six surfactants within a planar PNIPAM brush system, elucidating the polymer conformation, thermoresponse, and surfactant adsorption kinetics using ellipsometry, neutron reflectometry (NR), optical reflectometry and the quartz crystal microbalance technique. NR is used to measure the distribution of surfactants within the brush.
Findings: We find that only anionic surfactants modify the structure and thermoresponse of PNIPAM, with the greater affinity of anionic surfactants for PNIPAM (relative to cationic and nonionic surfactants) being the primary reason for this behaviour. These results show that the surfactant head–group has a

* Corresponding author.
E-mail address: s.prescott@unsw.edu.au (S.W. Prescott).
[1] Current address: The School of Chemistry, The University of Sydney, Australia.
[2] Current address: Department of Chemistry, The University of Sheffield, UK.

https://doi.org/10.1016/j.jcis.2022.10.071

more critical role in mediating PNIPAM-surfactant interaction than previously reported. Taking inspiration from prior molecular dynamics work on the PEO-surfactant system, we propose an interaction mechanism for PNIPAM and SDS that reconciles evidence for hydrophobic interaction with the observed head–group-dependent affinity.

1. Introduction

Polymer-surfactant systems are ubiquitous in commercial and industrial contexts, from personal care products to separation processes. Furthermore, polymer systems exhibiting stimuli-responsive behaviour are broadly applicable in the design of 'smart' systems, where the solution or interface properties can be controlled through a change in polymer conformation. It follows that understanding their interaction with surfactants is key to the application of responsive polymers in a wide range of systems. One common responsive polymer system is poly(*N*-isopropylacrylamide) (PNIPAM), which undergoes a swollen to collapsed transition in water as the system temperature is increased past its lower critical solution temperature (LCST) of 32 °C [1,2]. Surfactants have been reported to interact with PNIPAM, suppressing its thermoresponse; it is generally thought that hydrophobic forces drive this interaction [3–6]. However, it has been shown that only anionic surfactants affect the thermoresponse of PNIPAM [7–10], suggesting that the head–group also contributes. Understanding the complex interaction between PNIPAM and surfactants as a function of temperature and surfactant concentration will enable the application of responsive polymers in a broad range of contexts.

In this work, we study several anionic, cationic and nonionic surfactants, determining the surfactant's effect on, and affinity for, a PNIPAM polymer brush. We choose to study these interactions in the brush geometry for three reasons. Firstly, brushes can be studied with surface-sensitive techniques such as neutron reflectometry (NR), quartz crystal microbalance with dissipation monitoring (QCM-D), and ellipsometry, which allow for the direct study of polymer conformation and surfactant adsorption [11,12]. Secondly, the potential to affect the conformation of a PNIPAM brush with a small quantity of a specific molecule enhances its potential as an intelligent surface — surfactants, particularly sodium dodecylsulfate (SDS), are already known to modify the structure of PNIPAM [8,10,13] and similar neutral polymers [14,11]. Thirdly, studying tethered systems simplifies the control of surfactant concentration. In the planar brush geometry, the unbound surfactant concentration is essentially equal to the total surfactant concentration, allowing us to assume that the CMC of the surfactant within the systems studied is equivalent to that in a pure surfactant solution at 25 °C, denoted as $CMC^{\ominus}$.

1.1. Summary of prior work

The effects of certain surfactants on the thermotransition of PNIPAM have been documented in phenomenological studies for some time [10]. Anionic sulfate-headed surfactants strongly raise the LCST [10,15–18] and decrease the density [5,9,19,20,21] of PNIPAM at concentrations around their CMC for tail-lengths above 7 carbons [22]. Conversely, cationic ammonium-headed surfactants do not change the behaviour of PNIPAM at concentrations around their CMC for any tail-length [7,8]. Similarly, nonionic surfactants do not appreciably modulate the LCST of PNIPAM [7–10].

More detailed work (i.e., that examines system structure or polymer-surfactant affinity) has also been conducted, focusing on SDS as the model surfactant. Small angle neutron scattering (SANS) reveals that small SDS micelles form along the PNIPAM chain above the system critical aggregation concentration (CAC) [5,21]. Interestingly, the radius of the attached micelle increases with SDS concentration (to a maximum of ≈1.5 nm), while the distance between micelles (≈6 nm) remains constant. Similarly, time-resolved fluorescence quenching experiments [23] show that adsorbed SDS micelles increase in aggregation number from ≈8 to ≈22 as the free surfactant concentration increases from the CAC to the CMC. It has been confirmed via nuclear magnetic resonance spectroscopy (NMR) that no additional SDS is incorporated into the bound micelles at concentrations above its CMC [24]. These results imply that the number of micelles per chain is relatively constant and that more SDS either increases the number of solubilised PNIPAM chains or the micelle size. NMR has also revealed hints as to the interaction mechanism between PNIPAM and SDS, finding via nuclear Overhauser effect spectroscopy that the surfactant alkyl tail interacts with the PNIPAM isopropyl group [3]. The mass binding ratio (grams of SDS per gram of PNIPAM) at the CMC have been reported as 0.5 [5] (by gravimetric analysis), 0.6 [23] (by fluorescence quenching), and 8 [24] (by NMR). The reason for this large discrepancy is unclear; we will attempt to clarify this value in the current work.

It is clear from NMR, fluorescence techniques, and SANS that SDS forms distinct micelles along the PNIPAM backbone [24,3,6,23,5,21], as in the 'pearl-necklace model' first suggested by Shirahama et al. [25]. These adsorbed micelles are smaller than equivalent free micelles [23,5,21], with their aggregation number depending on free surfactant concentration [23,21]. It also seems that when the polymer undergoes a thermal collapse, micelles are released into bulk solution, rather than retained by the collapsed polymer [21,24]. In cases with a strong polymer-surfactant interaction (for instance, polyelectrolytes and oppositely charged surfactants) surfactants can interact with the polymer as single molecules, rather than micelles [26]. However, all evidence points to SDS-PNIPAM systems following the pearl-necklace mode of interaction [24,3,6,23,5,21].

1.2. Models for surfactant-PNIPAM interaction

Whilst the molecular structure of PNIPAM-SDS systems is well understood, the phenomenological studies of broader ranges of surfactants raise questions regarding the interaction mechanisms proposed. Many studies suggest the reason for the PNIPAM-surfactant affinity is the hydrophobic interaction between the aliphatic surfactant tail and the PNIPAM backbone and isopropyl carbons [3–6]. If this were true, then anionic and cationic surfactants would behave similarly. However, it is almost universally reported that SDS significantly influences the conformation and LCST of PNIPAM, whilst its cationic and nonionic counterparts have little or no measurable effect [10,22,8,9]. Due to these differences, it would seem that the mechanism through which anionic, nonionic and cationic (or at least sulfate, ethylene glycol and trimethylammonium headed) surfactants interact with PNIPAM must also differ, leading to the reasonable conclusion that the head–group plays an important role in driving the polymer-surfactant association.

This does not mean that the tail is not also important, only that the presence of a hydrophobic tail alone is not sufficient to induce significant interaction with PNIPAM.

There has been some debate about whether it is the size of the head–group [27,3–6] or the sign of its charge that is responsible for this discrepancy. The molecular dynamics simulations of Shang et al. [28] provide some insight into the nature of neutral, water-soluble polymer surfactant interaction, although they use PEO as their model polymer. They conclude that the polymer chain wraps around the micelles, shielding exposed hydrocarbon tails from the aqueous environment [29,28]. By swapping the charges of the SDS and DTAB in the simulation they convincingly show that it is the head–group charge, not size, that dictates the binding strength [28].

From a thermodynamic perspective, both the micellisation of surfactants [30,31] and thermal collapse of PNIPAM [1,32] are driven by the entropic penalty of hydrating the hydrophobic regions (the alkyl tail and isopropyl/backbone moiety, respectively). Surfactants suppress the thermoresponse of PNIPAM by replacing the water environment around its hydrophobic moieties with that of the micelle tails, thereby removing the driver of polymer collapse. Furthermore, when considering the micellisation of ionic surfactants, counterions must be bound to surfactant head–groups in order to stabilise the micelle. The condensation of these counterions carries an entropic penalty of its own. The polar amide moieties of PNIPAM could assist in stabilising the ionised surfactant head–groups without imposing an additional entropic penalty, as has been shown to be the case for polyelectrolytes [30,33]. The reduction in counterion condensation would help explain why anionic surfactants show a strong affinity for PNIPAM.

Despite hints as to the effect of the head–group on PNIPAM-surfactant interaction from PEO systems, we emphasise that the phenomenological experiments we review do not measure the affinity of the tested surfactants to the polymer, only their effect on its behaviour. Experiments that measure the structure of the polymer-surfactant system or associated binding ratios only study the anionic surfactant SDS. There is, therefore, no direct evidence that the surfactant head–group controls the interaction between the surfactant and PNIPAM - only that anionic surfactants have a greater effect on its thermoresponse. In this work, we will measure both the effect surfactants have on the conformation of a polymer brush, and their concentration within the brush layer. Through these measurements, we will demonstrate that prior observations of head–group dependent behaviour are due to changes in polymer-surfactant affinity, thereby showing that hydrophobic explanations of PNIPAM-surfactant behaviour are insufficient.

1.3. Effect of the brush geometry

The discussion above has focused on existing studies of PNIPAM-surfactant systems, which are generally conducted in solution or upon polymer microgels. The effect of confinement must be considered when translating solution-phase experiments to the brush geometry. For instance, inter-chain repulsion is more dominant in a brush than in a solution due to the proximity of neighbouring chains. This is comparable to a concentrated polymer solution or a polymer microgel but not identical, as the unoccupied space above the brush allows for anisotropic chain extension. There have only been two studies of the influence of surfactants on PNIPAM in the brush geometry, which examined the hydrodynamic radius of PNIPAM-coated silica nanoparticles in SDS [13,20]. The findings of these studies are in line with solution and microgel work, as outlined above and discussed in the Supporting Information. Work on interfacially adsorbed PNIPAM [19] as well as similar neutral planar polymer brush systems [14,11] have been able to resolve the changes in polymer structure as surfactant is added. Observed behaviour has been consistent with free-polymer behaviour in these systems. While more complex behaviour has been observed in polyelectrolyte systems with oppositely charged surfactants [12], we anticipate that the trends observed in free-polymer and microgel systems will translate to the brush geometry.

2. Materials and Methods

2.1. Materials

Native oxide silicon blocks (100 mm diameter, 10 mm thick) were used as brush substrates for NR experiments, whilst appropriately sized wafers were cut from native oxide silicon wafers (100 mm diameter, 1 mm thick) for ellipsometry experiments; wafers were purchased from EL-CAT Inc. (USA). Thermally treated silicon wafers with an oxide layer thickness of 82 nm (determined via ellipsometry) were used for fixed-angle optical reflectometry (FAOR) experiments. QSensor QSX 303 SiO_2 QCM-D sensors (Biolin Scientific) were purchased from ATA Scientific and cleaned before use by 30 seconds of plasma treatment followed by washing in 2 wt% SDS, rinsing with MilliQ water, and drying under nitrogen. Reagents used in the synthesis of the PNIPAM brushes are detailed in the Supporting Information.

The surfactants cetyltrimethylammonium bromide (CTAB, >=99%), dodecyltrimethylammonium bromide (DTAB, >=98%), hexaethyleneglycol monododecyl ether ($C_{12}E_6$, >=98%), sodium dodecylbenzenesulfonate (SDBS technical grade), dodecylpyridinium chloride (DPyC, >=98%) and SDS (>=98%) were purchased from Sigma Aldrich. SDS was recrystallised in ethanol before use, while the remaining surfactants were used as received. The deuterated surfactants dSDS and dCTAB were purchased from Cambridge isotope laboratories and used as received. $dC_{12}E_5$ was synthesised at the Oxford Deuteration Facility (STFC). The chemical structures of the surfactants used in this work, and a brief literature review of their $CMC^{\ominus}$ as a function of temperature, is included in the Supporting Information. $CMC^{\ominus}$ values and degrees of ionisation are summarised in Table 1.

2.2. Polymer synthesis

PNIPAM brushes were grafted-from silicon substrates via activators regenerated by electron transfer atom transfer radical polymerisation (ARGET-ATRP) [49,50], as per the protocol of Humphreys et al. [51]; full details of the method are included in the Supporting Information. For NR modelling, brushes are characterised by their interfacial volume ($\widehat{V}_I$), which is the volume of polymer per unit area, with units of length [52]. The dry thickness and interfacial volume of the brushes used in this work are detailed in Table 2.

Table 1
Critical micelle concentrations and degrees of ionisation (α) of the surfactants used in this work in pure water at 25 °C. For the temperature dependence of the CMC see Figure S2.

surfactant	$CMC^{\ominus}$ / mM		α	
SDS	8.07	[34–37]	0.26	[38,39]
SDBS	2.83	[40,41]	0.76	[42,43]
DTAB	14.80	[43,44]	0.21	[44]
CTAB	0.93	[34]	0.23	[38]
DPyC	16.95	[45]	0.38	[46,47]
$C_{12}E_5$	0.06	[48]	–	
$C_{12}E_6$	0.07	[36,48]	–	

Table 2
Dry thickness of the brush samples used in this work.

Sample	wafer type	Dry thickness (nm) Ellipsometry	NR	$\hat{V}_I$ (nm)
A	100 mm block	12.9 ± 0.3*	12.3	11.2
B	100 mm block	13.3 ± 0.2*	13.2	11.6
C	20 mm wafer	19.6 ± 0.2†	–	≈ 18§
D	20 mm wafer	60.94 ± 1.4†	–	≈ 55§
E	QCM-D sensor	≈ 13‡	–	≈ 12§
F	QCM-D sensor	≈ 20‡	–	≈ 18§
G	thermal oxide wafer	15 – 17	–	$\approx 15 - 17$§

§ Interfacial volume cannot be directly calculated using ellipsometry; values are approximated as 90% of the dry thickness, according to our previous work [52].
‡ Approximated from a sibling wafer synthesised in the same reaction mixture.
† Taken from 5 points over the wafer surface. Error is the standard deviation.
* Taken from 16 measurements over a 40 × 40 mm area in the centre of the wafer, see Figure S7. Error is the standard deviation.

2.3. Fixed angle optical reflectometry

FAOR was conducted in an impinging-jet flow geometry as described by Dijt et al. [53]. To increase sensitivity FAOR measurements were performed on silicon wafers with a thick 82 nm silica layer formed by thermal oxidation (Sample G, Table 2) [53]. A full description of the analysis method is included in the Supporting Information.

The geometry of the FAOR cell makes the technique ideally suited to study adsorption kinetics, as the measurement is carried out at the stagnation point. Measuring at the stagnation point means that solvent-exchange over the illuminated area is extremely rapid and as such can be used to accurately measure surfactant adsorption kinetics [54,55]. Figure S4 shows that the approach to equilibrium is fast, occurring over ≈3 min at 0.5×CMC$^{\ominus}$ and within a few seconds at 2×CMC$^{\ominus}$. As all other measurements in this study were given at least twenty minutes to equilibrate upon a change in surfactant condition, we are confident that all results reported here are indeed at equilibrium.

2.4. Ellipsometry

A Woollam M-2000 spectroscopic ellipsometer was used for the ellipsometry studies in this work. Dry measurements were taken between 60 and 75° inclusive at 5° intervals. Solvated spectroscopic ellipsometry measurements were performed at 75° with the sample contained in a Woollam 5 mL heated horizontal liquid cell atop a Woollam HLC-100 heating stage that provided temperature control. Temperature-dependent measurements were performed as a function of increasing temperature (i.e., low to high), with a thermal equilibration time of 35 min at each step. Solution changes were made by pumping at least 50 mL of fresh solution through the cell. For solution changes where a different surfactant was used the cell was flushed with 100 mL of MilliQ water before the injection of the new solution. Measurements were performed under static conditions once the solution exchange was completed. Samples C and D were studied with ellipsometry; details relating to data analyses are documented in the Supporting Information.

2.5. QCM-D

QCM-D studies were performed using a QSense Analyzer (Biolin Scientific) and 5 MHz QSensor QSX 303 SiO_2 sensors, with measurements carried out as a function of surfactant concentration and temperature. In all experiments all four cells in the QSense analyser were utilised, two cells contained blank silica-coated sensors, while the remaining cells contained samples E and F. The cells were connected in parallel and filled with identical solutions, using a peristaltic pump with a rate of 0.3 mL min^{-1} and a minimum pumped volume of 1.5 mL. All experiments began in MilliQ water, and were not commenced until all sensor frequencies exhibited less than 0.1 Hz min^{-1} drift; this typically occurred around an hour after the cells were filled. Surfactant concentration sweeps were always conducted from low to high concentration, and sensors and tubing were washed with ethanol before surfactant identity was changed. Temperature sweeps were conducted from low to high with a minimum equilibration time of 20 min and were monitored through the built-in thermostat. Temperature effects on sensor frequency were accounted for via the method outlined in the Supporting Information (Figure S14). All reported Δf values have already been divided by the harmonic number; this is done automatically by the QSense monitoring software.

2.6. Neutron reflectometry

Specular neutron reflectometry measurements were conducted using the Platypus reflectometer at the 20 MW OPAL reactor (ANSTO, Sydney) [56]. Measurements were made at angles of 0.6 and 3.6° for dry samples and 0.8 and 3.5° for solvated samples, yielding useful data within Q-ranges of 0.0073 to 0.31 Å^{-1} and 0.0096 to 0.31 Å^{-1} respectively. Choppers 1 and 4 were used for all experiments, and data reduction was performed using *refnx* following the standard procedure for Platypus [56], producing a final resolution of $\Delta Q/Q = 8.8\%$. Solvated experiments were carried out in standard solid–liquid cells (silicon backed) sandwiched between two heat-exchange plates, the temperature of which were controlled by a Julabo FP50-HE heater/chiller unit. The experiments were performed in D_2O–deuterated surfactant solutions to maximise contrast between the brush and the solvent, and in water contrast-matched to the SLD of PNIPAM (19.7 vol% D_2O, balance H_2O — hence referred to as CM) to highlight scattering from deuterated surfactants (see Table S4 for SLDs). Previously, PNIPAM has been observed to behave similarly in H_2O and D_2O, as measured by ellipsometry and NR, respectively; as such, it is expected that isotope effects will be of secondary importance here [57,51]. Hydrogenous surfactant was not used in any of the NR experiments as it would have interfered with the determination of brush structure (in D_2O) and not been visible in CM solution.

Two PNIPAM brush coated wafers were used for the NR measurements. This was done to increase throughput during the NR beamtime and prevent complexation between cationic and anionic surfactants. One wafer was used for SDS and $C_{12}E_5$ measurements, while the other was used for CTAB measurements. Both wafers were synthesised using the methodology described above and detailed in the Supporting Information, and both wafers had similar $\hat{V}_I$ (Table 2).

Collected NR data were analysed using the *refnx* reflectometry analysis package [58]. In keeping with our previous work [52], we enforce monotonicity (i.e., volume fraction must decrease as

distance from the substrate increases) for samples in pure D_2O, as no theoretical justification for non-monotonicity in neutral polymer brush profiles exists. However, it has recently been shown that non-monotonic volume fraction profiles can arise in more complicated or non-homogeneous systems [59–61]. As such, non-monotonicity was allowed in our model when a surfactant was present in the system. A modified freeform profile was used to analyse the NR data collected from deuterated surfactants in CM solution. In this modified model, the extent of the freeform profile was fixed based on the corresponding D_2O contrast data and volume fraction knots were defined absolutely (as opposed to being relative to the previous knot). A thorough explanation of the model, including a schematic of the volume fraction and SLD profiles, is included in the Supporting Information.

3. Results and discussion

We first investigate the effect that surfactants have on the structure and thermoresponse of a PNIPAM brush, before proceeding to measure the amount of surfactant that adsorbs within the brush. Throughout this section we report surfactant concentration relative to its CMC in pure water at 25 °C (denoted as $CMC^{\ominus}$, values in Table 1). This assumption is valid, as even for the highest polymer to surfactant volume ratio experiment (nonionic NR study), the number of moles of surfactant in the exchanged solution were an order of magnitude higher than the number of polymer repeat units. It is important to note that the CMC is a function of system temperature, so care must be taken when examining behaviour in systems where the temperature varies. The CMC of the surfactants used in this work has previously been investigated over the temperature range we cover here [34,35,62,36,63,37,43,40,64,47,44,45,48]. A summary of prior work is provided in Figure S2. The CMC values for the surfactants studied do not change by more than 15% over the temperature range investigated here.

3.1. Structural response of PNIPAM to different surfactants

Here, ellipsometry was used to measure the LCST of PNIPAM brushes as a function of surfactant identity and concentration. Ellipsometry measurements were carried out on two brushes, with thicknesses of 20 and 61 nm (Samples C and D), which allows for a brief investigation into the effect of polymer molecular weight on the PNIPAM-surfactant interaction. Different modelling techniques were required for each brush thickness, as detailed in the Supporting Information. The LCST is taken as the centre of the sigmoidal fit to the plots of thickness against temperature, as is standard for such analyses [51]. Fig. 1 is derived from the thickness vs. temperature plots shown in Figures S5 and S6. The thermoresponse was considered suppressed (i.e., no observable LCST) when there was no decreasing inflection in the fitted sigmoidal profile.

Fig. 1 reveals that anionic surfactants have a drastic effect on the thermoresponse of PNIPAM, whilst nonionic and cationic surfactants do not. The anionic surfactants SDS and SDBS completely suppressed the collapse of the PNIPAM layer over the investigated temperature range at concentrations in excess of $1\times CMC^{\ominus}$. Conversely, $C_{12}E_6$, DTAB, DPyC and CTAB did not appear to shift the transition temperature from its nominal aqueous value of 32 °C (Fig. 1) by more than a few degrees. The brush thickness was not a factor in the overall behaviour of the polymer-surfactant system; both brushes exhibited a swelling ratio (wet thickness divided by dry thickness) of ≈6 at $1\times CMC^{\ominus}$ SDS and 25 °C. Similarly, the brush thickness did not change the (negligible) effect of cationic surfactants. Patel et al. [7] show that polymer molecular weight can affect the interaction of PNIPAM with cationic and anionic surfactants for low molecular weight (<12 kDa) polymers. The polymers here have molecular weights of approximately 200 to 600 kDa[3]; for polymers of this size, molecular weight does not appear to have a significant effect on the interaction of PNIPAM with surfactant.

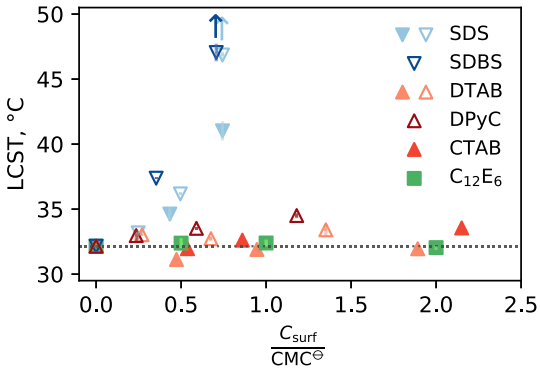

Fig. 1. Ellipsometrically determined LCST of Samples C (filled symbols) and D (hollow symbols), derived from fitting a sigmoid to ellipsometric thickness against temperature (see Figures S5 and S6). Anionic surfactants (SDS and SDBS) dramatically raise the LCST of PNIPAM; such behaviour is not observed for cationic (DTAB, DPyC or CTAB) and nonionic ($C_{12}E_6$) surfactants. The vertical arrows indicate that the brush did not exhibit a LCST in the temperature range probed at surfactant concentrations above this point.

Further insight into the effect of surfactant on the conformation of PNIPAM brushes is provided by NR. The volume fraction profiles shown in Fig. 2 are derived from NR experiments of hydrogenous polymer brushes in deuterated surfactant–D_2O solutions. We studied the structure of the system at $0.5\times CMC^{\ominus}$ and $2\times CMC^{\ominus}$ for SDS, and $2\times CMC^{\ominus}$ for CTAB and $C_{12}E_5$. The SDS values were chosen such that they were below and above the CMC, respectively, regardless of the effect of temperature (see Figure S2). $0.5\times CMC^{\ominus}$ measurements were omitted for the nonionic and cationic surfactants, as our ellipsometry experiments (Fig. 1) indicated that they had no meaningful effect on the brush structure below their CMC.

We first discuss the features evident in the reflectometry data, shown in the insets of Fig. 2, before discussing the output of the modelling. In water, the reflectometry data transition from profiles without strong features (25 °C), to profiles exhibiting two distinct Kiessig fringes (40 °C). The reflectometry profiles collected from SDS systems do not follow the same trend as the pure D_2O profiles. At $0.5\times CMC^{\ominus}$ of SDS the profile lacks strong features at both 25 and 32 °C, indicating that the layer remains swollen at both conditions. The fringe spacing at 40 °C is less well defined than in pure water. At $2\times CMC^{\ominus}$ of SDS the reflectometry profile is independent of temperature, most closely resembling the water profile at 25 °C. These reflectometry profiles suggests that SDS causes layer swelling at $0.5\times CMC^{\ominus}$ and completely suppresses the thermoresponse of PNIPAM at $2\times CMC^{\ominus}$, consistent with the ellipsometry experiments in Fig. 1. Reflectometry profiles collected from PNIPAM in $2\times CMC^{\ominus}$ $C_{12}E_5$ (Fig. 2d, inset) and CTAB (Fig. 2e, inset) solutions follow a similar trend to the pure D_2O profiles, strongly suggesting that these surfactants do not significantly change the polymer brush's structure.

The reflectometry profiles discussed above were analysed using the freeform modelling method documented in our earlier work [52] (the dataset from Fig. 2a was used as the exemplar dataset in that work). The modelled profiles support the interpretation drawn from the reflectometry data in the above paragraph. PNIPAM is more swollen in $0.5\times CMC^{\ominus}$ SDS than in water, while the thermoresponse is completely suppressed at $2\times CMC^{\ominus}$. The

[3] From the results of Murdoch et al. [57], assuming that molecular weight scales linearly with dry brush thickness

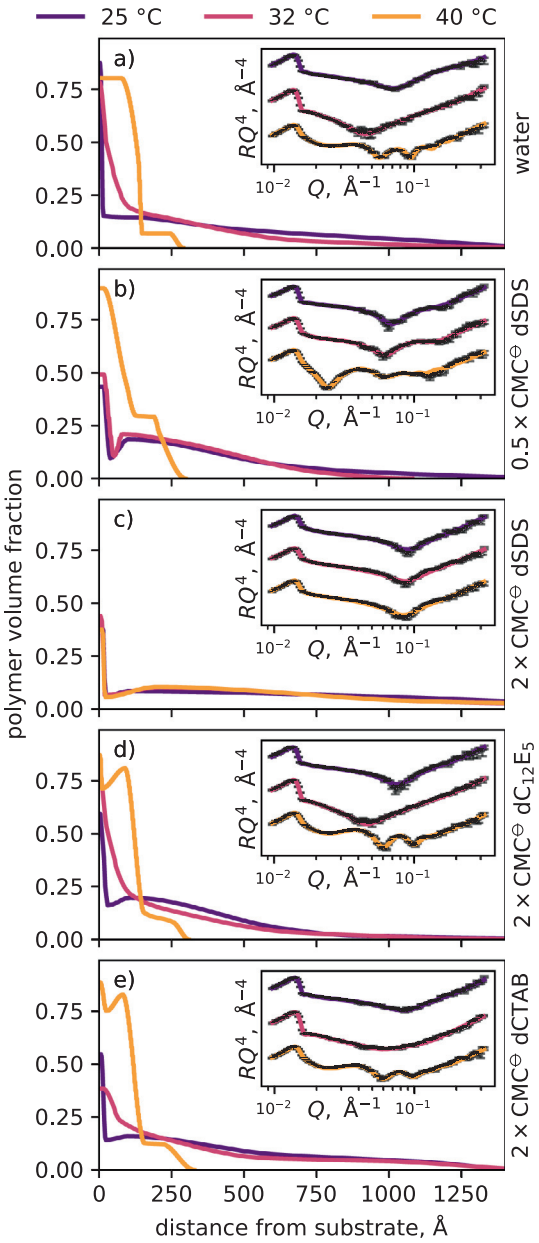

Fig. 2. Polymer volume fraction profiles at 25, 32 and 40 °C with (inset) corresponding modelled NR profiles and collected data. The solvent environment for each set is as follows (a) pure D_2O, (b) 0.5×CMC$^{\ominus}$ dSDS, (c) 2×CMC$^{\ominus}$ dSDS, (d) 2×CMC$^{\ominus}$ $dC_{12}E_5$ and (e) 2×CMC$^{\ominus}$ dCTAB; in all conditions the solvent is D_2O. The temperature dependence of the CMC for equivalent hydrogenous surfactant systems is shown in Figure S2. The NR profiles (*inset*) are vertically offset for clarity. Measurements in (a-d) were carried out on the same wafer ($V_l = 11.2$ nm), measurement in (e) was carried out on a sister wafer ($V_l = 11.6$ nm), control measurements are shown in Figure S8. Data and profiles in panel (a) are reproduced from the work of Gresham et al. [52], where they served as an exemplar dataset. Expanded reflectometry profiles are included in Figure S12.

thermoresponse of PNIPAM in other surfactants is mostly unchanged. The freeform modelling process does, however, reveal two features that are worthy of further discussion. Firstly, the presence of all surfactants at 2×CMC$^{\ominus}$ and 25 °C appear to reduce the volume fraction of the substrate-proximal layer. This substrate-proximal layer has been previously observed in NR studies of PNIPAM brushes [57], and is thought to consist of physisorbed segments of the PNIPAM brush. The reduction of the layer volume-fraction upon the addition of surfactant indicates that the surfactant is displacing PNIPAM at the silica–polymer interface. The second interesting feature in the modelled profiles is the lack of significant non-monotonicity in the collapsed brush systems (Fig. 2b-e). Previous NR work on polyelectrolyte copolymer brushes has shown that the analysis method used here is capable of accounting for significant non-monotonicity due to an uneven distribution of charge throughout the brush [60,61,65]. No such significant non-monotonicity is observed here, indicating that the distribution of surfactant is reasonably consistent throughout the brush. Small polymer-depleted regions are observed close to the substrate, perhaps due to the aforementioned adsorption of surfactant at the silica–polymer interface. Regardless, these polymer-depleted regions are small features that do not meaningfully change our interpretation of the reflectometry data.

3.2. Adsorption of surfactant within the PNIPAM layer

We now turn from the effects of various surfactants on a PNIPAM brush to an examination of surfactant adsorption within the brush. Here we use FAOR supported by QCM-D to approximate the adsorbed amount of surfactant, and NR to determine the distribution of surfactant within the brush layer.

QCM-D measurements at 20 °C are presented in Fig. 3, which show the change in frequency, Δf, and the change in dissipation, ΔD, as a function of surfactant concentration and identity for the 3rd, 5th, and 7th harmonic. Fig. 3 reveals that Δf and ΔD are much greater in magnitude upon the addition of SDS than CTAB or $C_{12}E_6$. A negative Δf and positive ΔD, as seen for SDS, are indicative of a swelling brush [51]. Conversely, a negative Δf and a ΔD of zero, as seen for CTAB and $C_{12}E_6$, is indicative of adsorption within the brush layer without any change in brush swelling — one explanation for these observations is that CTAB and $C_{12}E_6$ are adsorbing at the silica-polymer interface. We note that the collected Δf and ΔD signal for CTAB and $C_{12}E_6$ on the PNIPAM sensors were similar to the signal collected from bare silica (shown in Figure S15). The similarity between the PNIPAM brush and a bare silica surface for CTAB and $C_{12}E_6$ indicates that the results shown in Fig. 3 can be explained by adsorption of CTAB and $C_{12}E_6$ at the substrate (rather than adsorption into the polymer layer). An alternative explanation could be that the change in solution viscosity are responsible for the Δf and ΔD signals; a change in ionic strength can not explain the behaviour as $C_{12}E_6$ is nonionic. However, CTAB and $C_{12}E_6$ are present at very low concentrations and are expected to have a negligible impact on the solution viscosity (<0.3% for CTAB [66]) over the concentrations studied.

Furthermore, examining the differences between the harmonics in Fig. 3 also supports the substrate-adsorption model. Higher harmonics do not penetrate as far into the brush layer, and as such are sensitive to different regions within the brush than lower harmonics [67]. For SDS, the change in frequency decreases at higher harmonics, which indicates that mass is adsorbing a considerable distance from the substrate, i.e., within the brush periphery. A greater increase in mass in the brush periphery is consistent with a swelling polymer brush. Conversely, the frequency and dissipation do not change as a function of harmonic number with the addition of CTAB and $C_{12}E_6$, indicating that there is no layer swelling and that the adsorbed mass is concentrated at the base of the brush (detectable by all harmonics). This substrate interaction is not surprising, as both CTAB and $C_{12}E_6$ have been shown to adsorb to silica surfaces [68,69].

The behaviour of the PNIPAM-SDS system as a function of temperature was also investigated by QCM-D, with results shown in Fig. 4. The addition of SDS results in a significant decrease in Δf and increase in ΔD for the PNIPAM coated QCM-D wafer at 20 °C (as in Fig. 3). As temperature increases in pure water, a positive Δf and negative ΔD indicate a collapsing brush. As surfactant concentration is increased this trend disappears, with Δf and ΔD

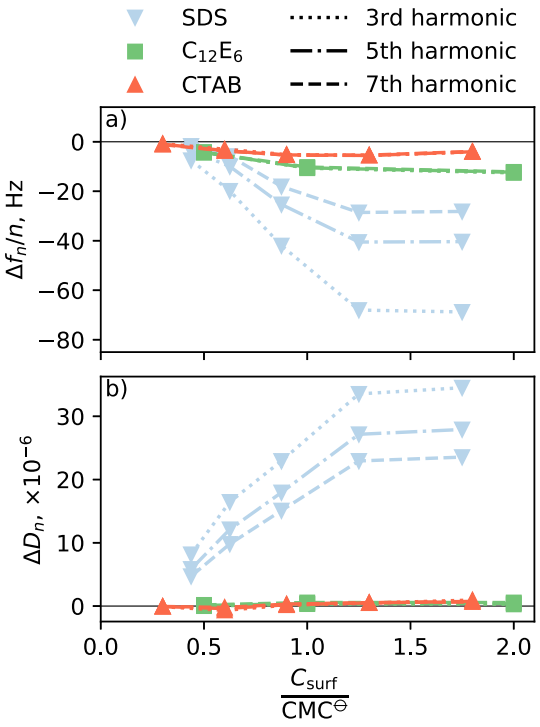

Fig. 3. Change in (a) normalised frequency and (b) dissipation of harmonics 3, 5 and 7 for a 13nm PNIPAM brush as a function of surfactant concentration and identity at 20 °C. Δf and ΔD are reported relative to the 1 mM $NaNO_3$ condition, and Δf values are divided by the harmonic number. All harmonics are shown for all surfactants, but are identical for cationic and nonionic surfactants. The addition of SDS causes significant changes in both Δf and ΔD, while CTAB and $C_{12}E_6$ induce only small changes in Δf. This indicates that SDS causes PNIPAM to swell, while CTAB and $C_{12}E_6$ do not. In Figure S15 is can be seen that the Δf and ΔD values for CTAB and $C_{12}E_6$ are similar for both the PNIPAM brush and bare silica substrate. Here CTAB is near its Krafft point, which is likely the reason that the signal plateaus before reaching 1×CMC$^{\ominus}$.

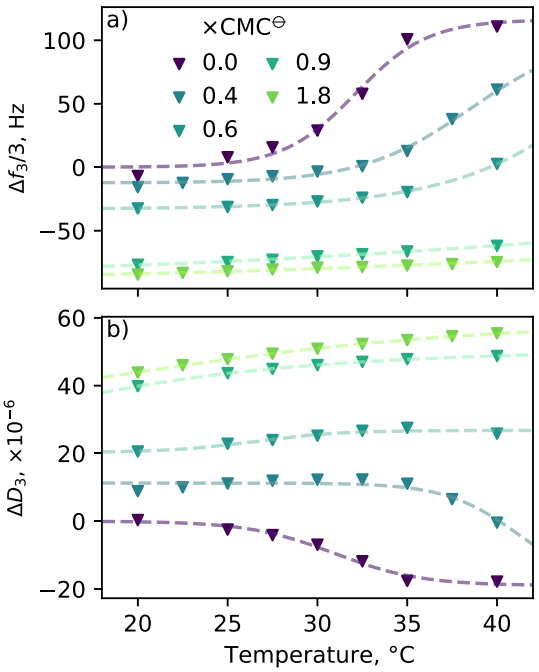

Fig. 4. Change in (a) Normalised frequency and (b) dissipation showing the thermoresponse of Sample E in SDS solutions relative to the CMC$^{\ominus}$. As temperature is increased in pure water Δf increases while ΔD decreases, corresponding to a layer that becomes less massive (the brush expels water as it collapses) and less mechanically coupled to the solvent. As SDS is added Δf decreases, while the ΔD increases, indicating that the brush is adsorbing mass (water or SDS) and swelling. Δf and ΔD are reported relative to the 1 mM $NaNO_3$ condition. The temperature correction method is documented in Figure S14.

values becoming relatively independent of temperature. This indicates that the layer swells as surfactant is added, and no longer undergoes a thermal collapse over the temperature range investigated — the same behaviour observed via ellipsometry (Fig. 1).

FAOR was used to provide further insight into the adsorption of surfactants within the brush layer. Fig. 5 shows the change in adsorbed mass as a function of surfactant concentration for several different surfactants; three key conclusions can be drawn from these results. Firstly, the adsorbed mass of surfactant increases linearly between the CAC and CMC$^{\ominus}$, and plateaus after the CMC$^{\ominus}$ is reached. Secondly, the adsorbed mass of anionic surfactants at 1×CMC$^{\ominus}$ is higher than comparable cationic or nonionic surfactants. Thirdly, the adsorbed mass of cationic and nonionic surfactants is non-zero; instead, they are approximately one-third of the value for the anionic surfactants. This third point implies that while all surfactants are concentrated within the brush layer (to some degree), only anionic surfactants have an appreciable effect on polymer conformation. However, we must stress here that the swelling of the PNIPAM layer during a FAOR experiment will lead to a reduction in the sensitivity (see Supporting Information), which will result in the calculated adsorbed amount of surfactant being underestimated relative to systems that do not swell; this is likely the case for the SDS system here.

Of course, if the polymer-surfactant system follows the pearl-necklace model, then the parameter of significance is the charge on the adsorbed micelles, which can be calculated from the mass of the adsorbed surfactant and the degree of ionisation (Table 1). Fig. 5b approximates the adsorbed charge for all surfactants stud-

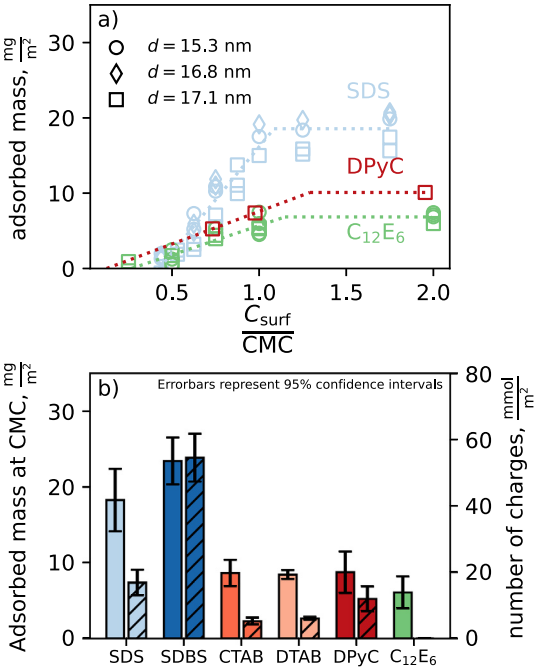

Fig. 5. FAOR results showing (a) adsorbed mass as a function of concentration for select surfactants, and (b) adsorbed mass (solid bars) and corresponding charge (dashed bars) for all surfactants above their CMC$^{\ominus}$. In (a) adsorption appears to scale linearly with surfactant concentration from the CAC up to the CMC$^{\ominus}$; the dotted lines are a guide to the eye. Panel (b) shows that the anionic surfactants examined exhibit much higher adsorbed masses than the nonionic and cationic surfactants. For both studies measurements were carried out on three different substrates with similar thicknesses, indicated by different marker symbols in (a).

ied based on the adsorbed mass, the surfactant molecular weight and the degree of ionisation. We find that the adsorbed charge (as determined by FAOR) is substantially higher for SDS than it is for CTAB (and obviously infinitely greater than for nonionic $C_{12}E_6$).

Now, we move on to examining the distribution of surfactant within the polymer layer through NR data collected from the CM system. Here, the primary contribution to the reflectometry profiles comes from surfactant adsorbed within the PNIPAM brush layer because the solvent (19.7 vol% D_2O, balance H_2O) SLD has been matched to the SLD of PNIPAM. As before, we first discuss the trend in the reflectometry profiles, shown in the insets of Fig. 6. In each inset two profiles are shown: that from the PNIPAM brush in pure CM (where there is only a small contribution from PNIPAM to the reflection pattern) and that from the PNIPAM brush in the deuterated surfactant-CM solution. The difference between these two reflection profiles emphasises that the presence of deuterated surfactant significantly changes the reflectivity.

The 0.5×CMC$^{\ominus}$ SDS sample (inset of Fig. 6a, b) displays minimal divergence from the pure CM sample at 25 °C, save for the development of a slight fringe at $Q = 0.1$ Å^{-1}. This fringe deepens as the sample is heated to 40 °C, which results in the reflectometry profile diverging further from that of the pure CM sample, indicating that surfactant is being concentrated in the collapsed brush layer. Interestingly, the fringe location does not change, only its depth, indicating that the corresponding feature changes in volume fraction, but not in thickness. The reflectivity of the 2×CMC$^{\ominus}$ SDS sample (inset of Fig. 6c, d) deviates significantly from the pure CM sample at both 25 and 40 °C. Surprisingly, the reflectivity from the 2×CMC$^{\ominus}$ $C_{12}E_5$ (Fig. 6e–f, e–f, inset) and CTAB (Fig. 6g–h, g–h, inset) samples also deviate from the pure CM sample. The 25 °C $C_{12}E_5$ and CTAB samples roughly resemble the 0.5×CMC$^{\ominus}$ 25 °C SDS data, while the 40 °C samples feature fringes that correspond to a ≈20 nm thick slab-like layer of surfactant. These profiles are remarkable, as no change was observed in the corresponding polymer-contrast profiles (Fig. 2d and 2e compared to 2a), meaning that surfactant is present within the layer without changing the structure of the layer.

The CM datasets were modelled with a modified version of the freeform profile used for the brush, detailed in the Supporting Information. Parallel Tempered Markov Chain Monte Carlo (PTMCMC) [71,72] sampling was used to determine the distribution of profiles that provided acceptable fits to the data. A description of the PTMCMC method can be found in our previous work [52], while details of its application to the datasets at hand can be found in the Supporting Information (Figure S10). For many of the datasets in Fig. 6 multiple families of profiles were found that adequately matched the collected data (Figure S10). From these families, only one was found that approximately matched the adsorbed amount of surfactant indicated by FAOR and QCM-D; the profile of best fit from the family that matched additional experiments were selected for presentation. Incorporating the adsorbed amount of surfactant into the model as an additional prior distribution (as was done for the polymer contrast) was not possible here, as layer thickness was encoded instead. Utilising our knowledge of the adsorbed amount in the selection of the prior profile achieves the same outcome.

The accepted profiles are presented in Fig. 6, with corresponding SLD profiles included in Figure S11. These profiles show where in the brush the surfactant is located, and allow us to calculate the volumetric binding ratio in the bulk of the brush. There is very little surfactant observed in the 0.5×CMC$^{\ominus}$ SDS, 2×CMC$^{\ominus}$ $C_{12}E_5$ or 2×CMC$^{\ominus}$ CTAB sample at either 25 or 40 °C. At these conditions, modelling reveals an enriched surfactant region near the substrate, with a uniform distribution of surfactant throughout the rest of the layer. At 40 °C the surfactant seems to be expelled from the polymer layer, as the surfactant:polymer volume ratio is much higher at 25 °C than 40 °C. As might be expected, the surfactant volume fraction is highest in the case of 2×CMC$^{\ominus}$ SDS. An SDS-enriched region is observed near the interface, while the volume fraction of SDS is proportional to that of the polymer throughout the bulk of the brush, with a volumetric binding ratio is approximately 1. We stress that the similarity between the polymer and surfactant volume fraction profiles across all measurements is not due to a poor contrast match or a change in PNIPAM deuteration state, as the control measurements (in black, Fig. 6) were done immediately before the CTAB and $C_{12}E_5$ measurements, with all surfactant solutions using the same CM precursor.

The NR results (Fig. 6) along with the FAOR results (Fig. 5) yield estimates of the binding ratio between the surfactant and the polymer, as shown in Fig. 7. Above the CMC$^{\ominus}$, the SDS:PNIPAM (mass) binding ratio is approximately 1.3, which is similar to the values reported by Mylonas et al. [23] and Mears et al. [5], (0.6 and 0.5, respectively). The difference can be explained by the sensitivity of CM NR to all polymer-proximal surfactant, rather than just bound surfactant. Similarly, the higher binding ratio of Chen et al. [3] (≈8) could be due to the sensitivity of their diffusion NMR to all surfactant that is mechanically coupled to the polymer (which would be higher in the untethered-polymer case than in a brush). It is interesting to note that in the case of polymer-surfactant systems where the surfactant has not suppressed the thermoresponse of the polymer (i.e. CTAB, $C_{12}E_6$, and low concentration SDS), the binding ratio is seen to reduce markedly as a function of temperature, which may be interpreted as the surfactant being expelled from the brush during this transition. For the system with 2 × CMC$^{\ominus}$ SDS, the surfactant:polymer ratio in the layer is unchanged with temperature and the thermoresponse of the polymer is correspondingly suppressed.

3.3. Effect of surfactant head–group

Ellipsometry, QCM-D and NR convincingly show that anionic surfactants affect both the structure and thermoresponse of PNIPAM in the brush geometry. Such behaviour has been reported previously for untethered PNIPAM [21,8,5,8,73,10,23,7] and nanoparticle-grafted PNIPAM brushes [20]. As found in the untethered-polymer literature, we find that SDS at the CMC is able to completely suppress the thermoresponse of PNIPAM over the temperature range probed (here, 20 to 45 °C). We find that the effect of SDS on PNIPAM plateaus above the surfactant CMC; this plateau is not always observed in untethered-polymer literature [7], likely because these experiments were conducted below the polymer saturation point, so the C_{free} never reached the CMC. In contrast, the cationic and nonionic surfactants studied here have a negligible effect at concentrations around their CMC, agreeing with prior phenomenological studies [7,8,9,10,15].

We contribute to this body of literature by adding an elucidation of polymer-surfactant interaction through quantifying surfactant adsorption into the polymer layer. By quantifying both polymer conformation (the effect of the surfactant) and the presence of surfactant in the layer (the affinity of the surfactant for the polymer), we can unpick the mechanism behind the PNIPAM-surfactant interaction. The obvious question raised by literature and the above findings is this: Why do DTAB/CTAB/DPyC (cationic surfactants) have such a markedly different effect on the behaviour of PNIPAM compared to SDS/SDBS (anionic surfactant)? Prior work (that typically examines only SDS) has claimed that SDS interacts with PNIPAM through the surfactant tail group binding to the hydrophobic polymer backbone [24,4,5,10]. The interaction model indicates that DTAB, $C_{12}E_6$ and SDS would have similar affinities for PNIPAM, which would result in similar adsorbed amounts. How-

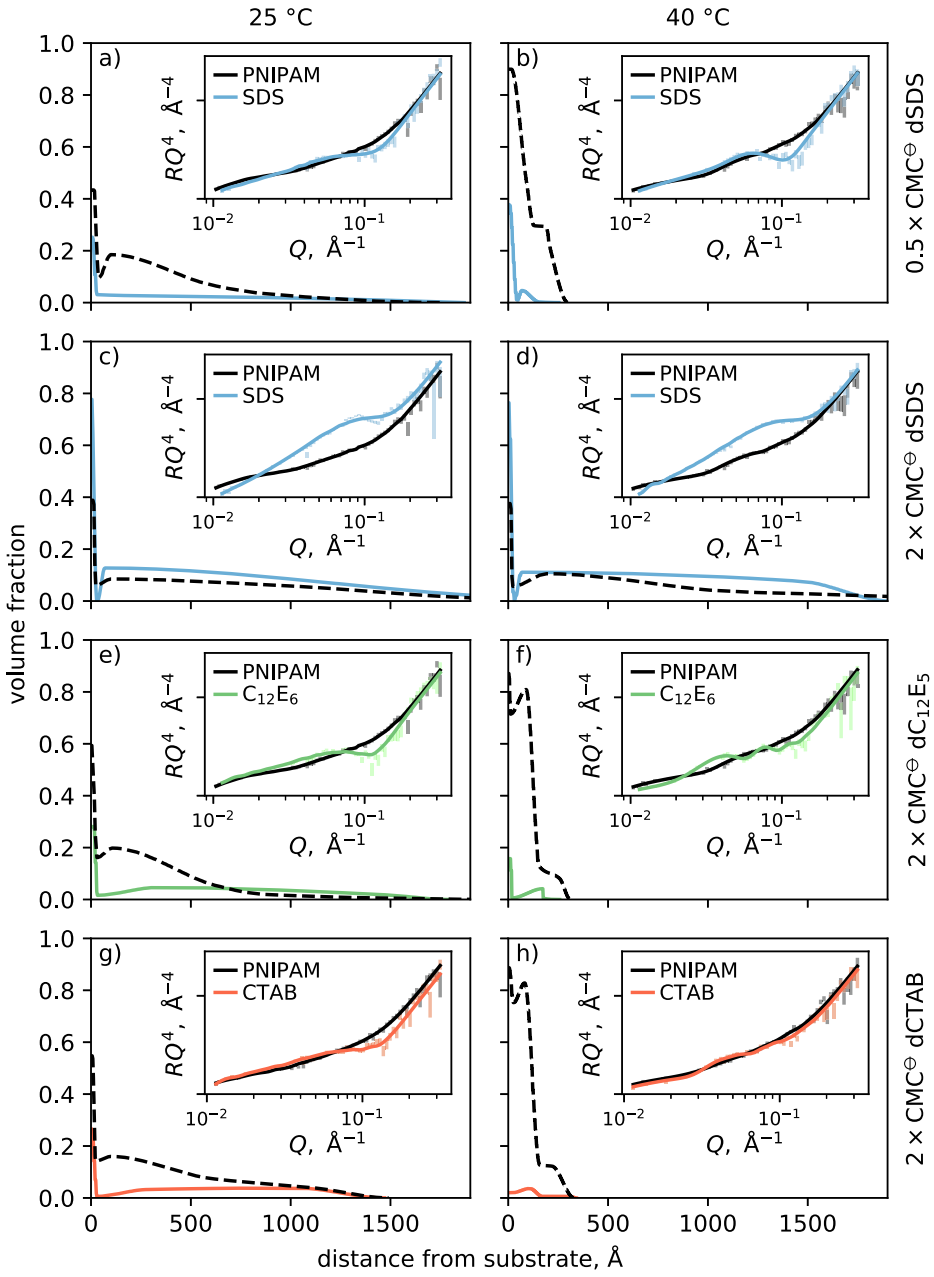

Fig. 6. SDS, $C_{12}E_5$ and CTAB volume fraction profiles derived from NR experiments where the solvent SLD is matched to that of PNIPAM, shown alongside PNIPAM volume fraction profiles (dashed black lines) from the D_2O measurements in Fig. 2 for reference. Reflectometry profiles are inset, and are shown against data from the pure CM system (black), to illustrate that there is a significant change in the reflectometry profile when surfactant is added. The modelled profiles show all surfactants appear to aggregate at the silica interface and associate with the polymer throughout the entire layer. SDS associates to a much greater degree than both $C_{12}E_5$ and CTAB. Model uncertainties are quantified in Figure S10 using our established method [70].

ever, our QCM-D, FAOR and CM NR experiments clearly show that SDS adsorbs in much greater amounts than the other surfactants. When considering the effects of surfactants on neutral polymers it is primarily the adsorbed charge, not the adsorbed mass, that dictates polymer conformation; both quantities are provided for surfactants above their CMC in Fig. 5b. The adsorbed charge is significantly lower for cationic surfactants compared to anionic surfactants, especially as the swelling induced by the latter will lead to their adsorbed mass being underestimated. Still, it is clear from both FAOR and QCM-D that there is some interaction between cationic surfactants and the PNIPAM brush. NR reveals the nature of this interaction, showing that, while some of the adsorption measured by other techniques is due to interaction with the substrate, both CTAB and $C_{12}E_5$ do interact with PNIPAM throughout the brush layer.

We conclude that the interaction between SDS and PNIPAM cannot be solely driven by the hydrophobic effect between the surfactant tail and the hydrophobic moieties on the polymer, as previous studies have suggested [4,6,24]. From Figs. 1, 3, 5, and 6, as well as other work [7,10,8], we see that the surfactant head–group plays a significant role in the interaction between PNIPAM and surfactants. This head–group dependent behaviour has been observed in molecular dynamics studies of the PEO-surfactant system [28,29,74,75]. We believe that the best model for PNIPAM-SDS interaction is one where the polymer binds to the surface of the surfactant micelle — the same mechanism proposed for SDS-PEO

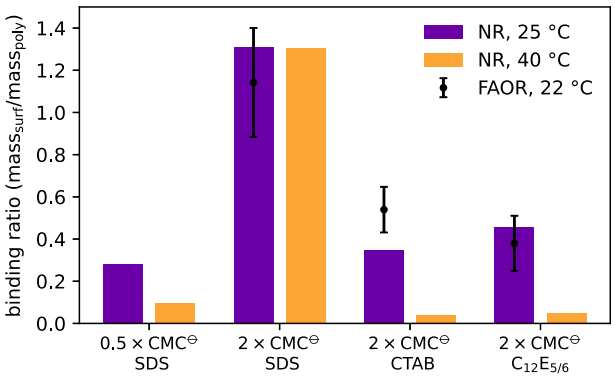

Fig. 7. The binding ratio between surfactant and polymer as estimated via FAOR and NR, as a function of temperature, surfactant concentration, and surfactant identity. For the systems that do not suppress the thermoresponse of the PNIPAM (CTAB, $C_{12}E_6$, and low concentration SDS), the binding ratio is seen to reduce considerably at higher temperatures where the collapsing brush expels the surfactant. With the higher concentration if SDS, the collapse is suppressed and the surfactant:polymer ratio is unchanged.

systems by Shang et al. [29]. In this model, the hydrophobic moieties of PNIPAM bind to the exposed regions of the micelle core, reducing the surface energy of the micelle. The binding of hydrophobic PNIPAM moieties to the micelle in this matter matches the NMR study of Chen et al. [4], which finds that SDS alkyl protons are near the isopropyl groups on the PNIPAM. Simultaneously, the PNIPAM amide forms ionic hydrogen bonds with the anionic sulfate head–group, explaining the head–group dependence observed here and elsewhere [7,8,10,18].

It appears that there is also a mechanism through which the local concentration of the surfactants studied here is increased in the presence of PNIPAM without strongly affecting polymer conformation. We draw this conclusion primarily from Fig. 5b and the surfactant volume fractions in Fig. 6, which show that cationic and nonionic surfactants are present in the brush layer at concentrations where SDS has some effect on the thermotransition. This fits with reports of cationic surfactants having a small effect on the behaviour of PNIPAM [7,10,76,77,78]. The mechanism behind this behaviour could be polymer-induced aggregation, the second mode of surfactant interaction observed by Walter et al. [6], where the presence of polymer increases the local concentration of surfactant by facilitating the formation of transitory surfactant aggregates below the CMC$^{\ominus}$. These surfactant aggregates are not strongly bound to the polymer, and hence do not strongly affect the polymer behaviour.

Finally, we also note that the magnitude of contribution of counterion condensation on the surfactant/polymer system changes with salt concentration; we will explore this for the PNIPAM/SDS/NaCl system in a future paper.

4. Conclusion

We have investigated the effects of anionic, cationic and nonionic surfactants on the behaviour of a PNIPAM brush, finding that only anionic surfactants induce swelling in, and suppress the thermoresponse of, PNIPAM. These finding are consistent with phenomenological studies of the untethered system [7,10,8]. Using QCM-D, FAOR and NR we have quantified the amount and distribution of surfactant adsorbed within the brush, revealing that the primary reason for the exceptional behaviour of the anionic system is that anionic surfactants have a greater affinity for PNIPAM. Contrast-varied NR indicates that the SDS:PNIPAM mass binding ratios of approximately 1:1 above the CMC$^{\ominus}$, agreeing reasonably well with the values reported by Mylonas et al. [23] and Mears et al. [5]. Conversely, we find binding ratios of cationic and nonionic surfactants to be much lower, approximately 0.2:1 at 25 °C. As part of this work, we have demonstrated that it is possible to determine the concentration profiles of an adsorbent within a polymer brush and developed new techniques for the analysis of such systems.

The difference we observe in the affinity between surfactant types implies that the polymer-surfactant interaction is mediated in-part by the head–group, and by extension the electrostatic interactions it undergoes, rather than exclusively by the tail as often reported [3,4,6,79]. We suggest that the PNIPAM-surfactant interaction is the same as the model proposed for PEO-surfactant systems. In this model, the polymer adsorbs onto the micelle surface, with the hydrophobic polymer moieties in contact with the hydrophobic surfactant tail, and the hydrophilic polymer moieties forming ionic hydrogen bonds with the surfactant head–group [28]. However, our results indicate that the amount of surfactant present within the layer can not completely account for the behaviour change, indicating that there may be a secondary mechanism through which PNIPAM increases the local concentration of surfactants that does not involve strong binding and subsequent swelling.

5. CRediT statement

Isaac Gresham: Methodology, Software, Validation, Formal analysis, Investigation, Writing – Original Draft, Writing – Review & Editing, Visualisation **Joshua D. Willott:** Methodology, Investigation, Writing – Review & Editing, Resources, Supervision **Edwin C. Johnson:** Investigation, Writing – Review & Editing **Peixun Li:** Resources **Grant B. Webber:** Writing – Review & Editing, Supervision, Funding acquisition, Resources **Erica J. Wanless:** Writing – Review & Editing, Supervision, Funding acquisition, Resources **Andrew R.J. Nelson:** Methodology, Software, Writing – Review & Editing, Supervision, Resources, Funding acquisition **Stuart W. Prescott:** Conceptualisation, Methodology, Software, Writing – Review & Editing, Supervision, Resources, Funding acquisition

Data availability

Data will be made available on Supplementary material: https://doi.org/10.5281/zenodo.7156760.

Declaration of Competing Interest

The authors declare that they have no known competing financial interests or personal relationships that could have appeared to influence the work reported in this paper.

Acknowledgements

This work was supported by ANSTO through an Australian Centre for Neutron Scattering Program Grant (PP4274). IJG and ECJ thank the Australian Government and AINSE Ltd. for providing financial assistance for the period when this work was completed (Research Training Program Scholarship and PGRA Award, respectively). Support from the Science and Technology Facilities Council (STFC) for the synthesis of the $dC_{12}E_5$ surfactant at the ISIS Deuteration Facility is gratefully acknowledged.

Appendix A. Supplementary material

Supplementary data associated with this article can be found, in the online version, at https://doi.org/10.1016/j.jcis.2022.10.071 and at https://doi.org/10.5281/zenodo.7156759.

References

[1] A. Halperin, M. Kröger, F.M. Winnik, Poly(*N*-isopropylacrylamide) phase diagrams: Fifty years of research, Angew. Chem. - Int. Ed. 54 (51) (2015) 15342–15367, https://doi.org/10.1002/anie.201506663.

[2] P. Liu, M. Freeley, A. Zarbakhsh, M. Resmini, Adsorption of soft NIPAM nanogels at hydrophobic and hydrophilic interfaces: Conformation of the interfacial layers determined by neutron reflectivity, J. Colloid Interface Sci. 623 (2022) 337–347, https://doi.org/10.1016/j.jcis.2022.05.010.

[3] J. Chen, H. Xue, Y. Yao, H. Yang, A. Li, M. Xu, Q. Chen, R. Cheng, Effect of surfactant concentration on the complex structure of poly(*N*-isopropylacrylamide)/sodium *n*-dodecyl sulfate in aqueous solutions, Macromolecules 45 (13) (2012) 5524–5529, https://doi.org/10.1021/ma301003r.

[4] J. Chen, J. Spěváček, L. Hanyková, NMR methods to study effects of additives on phase separation of thermoresponsive polymer, Macromolecular Symposia 339 (1) (2014) 24–32, https://doi.org/10.1002/masy.201300130.

[5] S.J. Mears, Y. Deng, T. Cosgrove, R. Pelton, Structure of sodium dodecyl sulfate bound to a poly(NIPAM) microgel particle, Langmuir 13 (7) (1997) 1901–1906, https://doi.org/10.1021/la960515x.

[6] R. Walter, J. Rička, C. Quellet, R. Nyffenegger, T. Binkert, Coil-globule transition of poly(*N*-isopropylacrylamide): A study of polymer-surfactant association, Macromolecules 29 (11) (1996) 4019–4028, https://doi.org/10.1021/ma951529x.

[7] T. Patel, G. Ghosh, S.-I. Yusa, P. Bahadur, Solution behavior of poly(*N*-isopropylacrylamide) in water: Effect of additives, J. Dispersion Sci. Technol. 32 (8) (2011) 1111–1118, https://doi.org/10.1080/01932691.2010.497701.

[8] M.S. Lee, J.-C. Kim, Effects of surfactants on phase transition of poly(*N*-isopropylacrylamide) and poly(*N*-isopropylacrylamide-co-dimethylaminoethylmethacrylate), J. Dispersion Sci. Technol. 33 (2) (2012) 272–277, https://doi.org/10.1080/01932691.2011.561181.

[9] B. Jean, L.T. Lee, Noninteracting versus interacting poly(*N*-isopropylacrylamide)-surfactant mixtures at the air-water interface, J. Phys. Chem. B 109 (11) (2005) 5162–5167, https://doi.org/10.1021/jp0454265.

[10] E. Kokufuta, Y.Q. Zhang, T. Tanaka, A. Mamada, Effects of surfactants on the phase transition of poly(*N*-isopropylacrylamide) gel, Macromolecules 26 (5) (1993) 1053–1059, https://doi.org/10.1021/ma00057a027.

[11] O. Artykulnyi, M. Avdeev, Y. Kosiachkin, V. Petrenko, I. Safarik, L. Bulavin, Neutron investigation of interaction between anionic surfactant micelles and poly (ethylene glycol) polymer brush system, Nuclear Physics and Atomic, Energy 22 (2021) 149–156, https://doi.org/10.15407/jnpae2021.02.149.

[12] M. Moglianetti, J.R.P. Webster, S. Edmondson, S.P. Armes, S. Titmuss, A neutron reflectivity study of surfactant self-assembly in weak polyelectrolyte brushes at the sapphire-water interface, Langmuir 27 (8) (2011) 4489–4496, https://doi.org/10.1021/la200211x.

[13] P.W. Zhu, L. Chen, Synergistic effects of bound micelles and temperature on the flexibility of thermoresponsive polymer brushes, J. Phys. Chem. B 120 (44) (2016) 11595–11606, https://doi.org/10.1021/acs.jpcb.6b08696.

[14] M. Yanez Arteta, F. Eltes, R.A. Campbell, T. Nylander, Interactions of PAMAM Dendrimers with SDS at the Solid-Liquid Interface, Langmuir 29 (19) (2013) 5817–5831, https://doi.org/10.1021/la400774p.

[15] C. Wu, S. Zhou, Effects of surfactants on the phase transition of poly(*N*-isopropylacrylamide) in water, J. Polym. Sci., Part B: Polym. Phys. 34 (9) (1996) 1597–1604, https://doi.org/10.1002/(SICI)1099-0488(19960715)34:9<1597::AID-POLB8>3.0.CO;2-I.

[16] B. Cabane, R. Duplessix, Organization of surfactant micelles adsorbed on a polymer molecule in water : a neutron scattering study, Journal de Physique 43 (10) (1982) 1529–1542, https://doi.org/10.1051/jphys:0198200430100152900.

[17] R.D. Groot, Mesoscopic simulation of polymer-surfactant aggregation, Langmuir 16 (19) (2000) 7493–7502, https://doi.org/10.1021/la000010d.

[18] D. Myers, Surfactant science and technology, Wiley, 2006, https://doi.org/10.1002/9781119465829.

[19] R.M. Richardson, R. Pelton, T. Cosgrove, J. Zhang, A Neutron Reflectivity Study of Poly(*N*-isopropylacrylamide) at the Air-Water Interface with and without Sodium Dodecyl Sulfate, Macromolecules 33 (17) (2000) 6269–6274, https://doi.org/10.1021/ma000095p.

[20] P.W. Zhu, Effects of sodium dodecyl sulfate on structures of poly(*N*-isopropylacrylamide) at the particle surface, J. Phys. Chem. B 119 (1) (2015) 359–371, https://doi.org/10.1021/jp510350w.

[21] L.-T. Lee, B. Cabane, Effects of surfactants on thermally collapsed poly(*N*-isopropylacrylamide) macromolecules, Macromolecules 30 (97) (1997) 6559–6566, https://doi.org/10.1021/ma9704469.

[22] H.G. Schild, D.A. Tirrell, Interaction of poly(*N*-isopropylacrylamide) with sodium *n*-alkyl sulfates in aqueous solution, Langmuir 7 (4) (1991) 665–671, https://doi.org/10.1021/la00052a013.

[23] Y. Mylonas, G. Staikos, P. Lianos, Investigation of the poly(*N*-isopropylacrylamide)-sodium dodecyl sulfate complexation with viscosity, dialysis, and time-resolved fluorescence-quenching measurements, Langmuir 15 (21) (1999) 7172–7175, https://doi.org/10.1021/la990155o.

[24] J. Chen, X. Gong, H. Yang, Y. Yao, M. Xu, Q. Chen, R. Cheng, NMR study on the effects of sodium n-dodecyl sulfate on the coil-to-globule transition of poly(*N*-isopropylacrylamide) in aqueous solutions, Macromolecules 44 (15) (2011) 6227–6231, https://doi.org/10.1021/ma201269u.

[25] K. Shirahama, K. Tsujii, T. Takagi, Free-boundary electrophoresis of sodium dodecyl sulfate–protein polypeptide complexes with special reference to SDS–polyacrylamide gel electrophoresis, The Journal of Biochemistry 75 (2) (1974) 309–319, https://doi.org/10.1093/oxfordjournals.jbchem.a130398.

[26] J. Merta, V.M. Garamus, R. Willumeit, P. Stenius, Structure of Complexes Formed by PDADMAC and Sodium Palmitate, Langmuir 18 (20) (2002) 7272–7278, https://doi.org/10.1021/la011867t.

[27] E. Ruckenstein, G. Huber, H. Hoffmann, Surfactant aggregation in the presence of polymers, Langmuir 3 (3) (1987) 382–387, https://doi.org/10.1021/la00075a019.

[28] B.Z. Shang, Z. Wang, R.G. Larson, Effect of headgroup size, charge, and solvent structure on polymer-micelle interactions, studied by molecular dynamics simulations, J. Phys. Chem. B 113 (46) (2009) 15170–15180, https://doi.org/10.1021/jp9057737.

[29] B.Z. Shang, Z. Wang, R.G. Larson, Molecular dynamics simulation of interactions between a sodium dodecyl sulfate micelle and a poly(ethylene oxide) polymer, J. Phys. Chem. B 112 (10) (2008) 2888–2900, https://doi.org/10.1021/jp0773841.

[30] A.J. Konop, R.H. Colby, Role of Condensed Counterions in the Thermodynamics of Surfactant Micelle Formation with and without Oppositely Charged Polyelectrolytes, Langmuir 15 (1) (1999) 58–65, https://doi.org/10.1021/la980782y.

[31] B.W. Barry, R. Wilson, C.M.C., counterion binding and thermodynamics of ethoxylated anionic and cationic surfactants, Colloid and Polymer Science 256 (3) (1978) 251–260, doi:10.1007/bf01550555.

[32] R. Pelton, Poly(*N*-isopropylacrylamide) (PNIPAM) is never hydrophobic, J. Colloid Interface Sci. 348 (2) (2010) 673–674, https://doi.org/10.1016/j.jcis.2010.05.034.

[33] J. Penfold, R.K. Thomas, Counterion Condensation, the Gibbs Equation, and Surfactant Binding: An Integrated Description of the Behavior of Polyelectrolytes and Their Mixtures with Surfactants at the Air-Water Interface, The Journal of Physical Chemistry B 124 (28) (2020) 6074–6094, https://doi.org/10.1021/acs.jpcb.0c02988.

[34] A. Cifuentes, J.L. Bernal, J.C. Diez-Masa, Determination of Critical Micelle Concentration Values Using Capillary Electrophoresis Instrumentation, Anal. Chem. 69 (20) (1997) 4271–4274, https://doi.org/10.1021/ac970696n.

[35] S.S. Shah, N.U. Jamroz, Q.M. Sharif, Micellization parameters and electrostatic interactions in micellar solution of sodium dodecyl sulfate (SDS) at different temperatures, Colloids Surf., A 178 (1–3) (2001) 199–206, https://doi.org/10.1016/S0927-7757(00)00697-X.

[36] E. Fegyver, R. Mészáros, The impact of nonionic surfactant additives on the nonequilibrium association between oppositely charged polyelectrolytes and ionic surfactants, Soft Matter 10 (12) (2014) 1953, https://doi.org/10.1039/c3sm52889h.

[37] J.P. Marcolongo, M. Mirenda, Thermodynamics of sodium dodecyl sulfate (SDS) micellization: An undergraduate laboratory experiment, J. Chem. Educ. 88 (5) (2011) 629–633, https://doi.org/10.1021/ed900019u.

[38] C. Vautier-Giongo, B.L. Bales, Estimate of the Ionization Degree of Ionic Micelles Based on Krafft Temperature Measurements, J. Phys. Chem. B 107 (23) (2003) 5398–5403, https://doi.org/10.1021/jp0270957.

[39] B.L. Bales, A definition of the degree of ionization of a micelle based on its aggregation number, J. Phys. Chem. B 105 (29) (2001) 6798–6804, https://doi.org/10.1021/jp004576m.

[40] S.K. Hait, P.R. Majhi, A. Blume, S.P. Moulik, A critical assessment of micellization of sodium dodecyl benzene sulfonate (SDBS) and its interaction with poly(vinyl pyrrolidone) and hydrophobically modified polymers, JR 400 and LM 200, J. Phys. Chem. B 107 (15) (2003) 3650–3658, https://doi.org/10.1021/jp027379r.

[41] A.K. Sood, M. Aggarwal, Evaluation of micellar properties of sodium dodecylbenzene sulphonate in the presence of some salts, Journal of Chemical Sciences 130 (4) (2018), https://doi.org/10.1007/s12039-018-1446-z.

[42] M. Khandelwal, J.S. Ampily, B. Rai, G. Sarasan, Thermodynamic Study of Micellization of SDBS in Aqueous and in Binary Solvent Systems of Ethylene Glycol, International Journal of Engineering Research and Technology 09 (06) (2020), https://doi.org/10.17577/ijertv9is060363.

[43] S. Chauhan, K. Sharma, Effect of temperature and additives on the critical micelle concentration and thermodynamics of micelle formation of sodium dodecyl benzene sulfonate and dodecyltrimethylammonium bromide in aqueous solution: A conductometric study, J. Chem. Thermodyn. 71 (2014) 205–211, https://doi.org/10.1016/j.jct.2013.12.019.

[44] S.K. Shah, S.K. Chatterjee, A. Bhattarai, The effect of methanol on the micellar properties of dodecyltrimethylammonium bromide (DTAB) in aqueous medium at different temperatures, J. Surfactants Deterg. 19 (1) (2016) 201–207, https://doi.org/10.1007/s11743-015-1755-x.

[45] J.J. Galán, A. Gonzáles-Pérez, J.L.D. Cactillo, J.R. Rodríguez, Thermal parameters associated to micellization of dodecylpyridinium bromide and chloride in aqueous solution, J. Therm. Anal. Calorim. 70 (1) (2002) 229–234, https://doi.org/10.1023/A:1020678222376.

[46] H. Akbaş, Ç. Batıgöç, Micellization of dodecylpyridinium chloride in water-ethanol solutions, Colloid Journal 70 (2) (2008) 127–133, https://doi.org/10.1134/s1061933x08020014.
[47] J. Mata, D. Varade, P. Bahadur, Aggregation behavior of quaternary salt based cationic surfactants, Thermochim. Acta 428 (1–2) (2005) 147–155, https://doi.org/10.1016/j.tca.2004.11.009.
[48] L.-J. Chen, S.-Y. Lin, C.-C. Huang, E.-M. Chen, Temperature dependence of critical micelle concentration of polyoxyethylenated non-ionic surfactants, Colloids Surf., A 135 (1–3) (1998) 175–181, https://doi.org/10.1016/S0927-7757(97)00238-0.
[49] K. Matyjaszewski, D. Hongchen, W. Jakubowski, J. Pietrasik, A. Kusumo, Grafting from surfaces for everyone: ARGET ATRP in the presence of air, Langmuir 23 (8) (2007) 4528–4531, https://doi.org/10.1021/la063402e.
[50] J.-S. Wang, K. Matyjaszewski, Controlled/living radical polymerization. atom transfer radical polymerization in the presence of transition-metal complexes, Journal of the American Chemical Society 117 (20) (1995) 5614–5615, https://doi.org/10.1021/ja00125a035.
[51] B.A. Humphreys, J.D. Willott, T.J. Murdoch, G.B. Webber, E.J. Wanless, Specific ion modulated thermoresponse of poly(*N*-isopropylacrylamide) brushes, PCCP 18 (8) (2016) 6037–6046, https://doi.org/10.1039/C5CP07468A.
[52] I.J. Gresham, T.J. Murdoch, E.C. Johnson, H. Robertson, G.B. Webber, E.J. Wanless, S.W. Prescott, A.R.J. Nelson, Quantifying the robustness of the neutron reflectometry technique for structural characterization of polymer brushes, J. Appl. Crystallogr. 54 (3) (2021) 739–750, https://doi.org/10.1107/s160057672100251x.
[53] J.C. Dijt, M.A. Cohen Stuart, J.E. Hofman, G.J. Fleer, Kinetics of polymer adsorption in stagnation point flow, Colloids Surf. 51 (C) (1990) 141–158, https://doi.org/10.1016/0166-6622(90)80138-T.
[54] R. Atkin, V.S.J. Craig, S. Biggs, Adsorption Kinetics and Structural Arrangements of Cationic Surfactants on Silica Surfaces, Langmuir 16 (24) (2000) 9374–9380, https://doi.org/10.1021/la0001272.
[55] R. Atkin, V.S.J. Craig, E.J. Wanless, S. Biggs, Mechanism of cationic surfactant adsorption at the solid–aqueous interface, Advances in Colloid and Interface Science 103 (3) (2003) 219–304, https://doi.org/10.1016/s0001-8686(03)00002-2.
[56] M. James, A. Nelson, S.A. Holt, T. Saerbeck, W.A. Hamilton, F. Klose, The multipurpose time-of-flight neutron reflectometer Platypus at Australia's OPAL reactor, Nucl. Instrum. Methods Phys. Res., Sect. A 632 (1) (2011) 112–123, https://doi.org/10.1016/j.nima.2010.12.075.
[57] T.J. Murdoch, B.A. Humphreys, J.D. Willott, K.P. Gregory, S.W. Prescott, A. Nelson, E.J. Wanless, G.B. Webber, Specific anion effects on the internal structure of a poly(*N*-isopropylacrylamide) brush, Macromolecules 49 (16) (2016) 6050–6060, https://doi.org/10.1021/acs.macromol.6b01001.
[58] A.R.J. Nelson, S.W. Prescott, *refnx*: neutron and X-ray reflectometry analysis in Python, J. Appl. Crystallogr. 52 (1) (2019) 193–200, https://doi.org/10.1107/S1600576718017296.
[59] E.C. Johnson, J.D. Willott, I.J. Gresham, T.J. Murdoch, B.A. Humphreys, S.W. Prescott, A. Nelson, W.M. de Vos, G.B. Webber, E.J. Wanless, Enrichment of charged monomers explains non-monotonic polymer volume fraction profiles of multi-stimulus responsive copolymer brushes, Langmuir 36 (42) (2020) 12460–12472, https://doi.org/10.1021/acs.langmuir.0c01502.
[60] E.C. Johnson, I.J. Gresham, S.W. Prescott, A. Nelson, E.J. Wanless, G.B. Webber, The direction of influence of specific ion effects on a pH and temperature responsive copolymer brush is dependent on polymer charge, Polymer 214 (November 2020) (2021) 123287, https://doi.org/10.1016/j.polymer.2020.123287.
[61] S. Bialas, T. Krappitz, S.L. Walden, K. Kalayci, D. Kodura, H. Frisch, J.M. MacLeod, A. Nelson, L. Michalek, C. Barner-Kowollik, Light-Gated Control of Conformational Changes in Polymer Brushes, Advanced Materials Technologies 7 (4) (2022) 2100347, https://doi.org/10.1002/admt.202100347.
[62] S.A. Markarian, L.R. Harutyunyan, R.S. Harutyunyan, The properties of mixtures of sodium dodecylsulfate and diethylsulfoxide in Water, J. Solution Chem. 34 (3) (2005) 361–368, https://doi.org/10.1007/s10953-005-3056-x.
[63] B. Naskar, A. Dey, S.P. Moulik, Counter-ion effect on micellization of ionic surfactants: a comprehensive understanding with two representatives, sodium dodecyl sulfate (SDS) and dodecyltrimethylammonium bromide (DTAB), J. Surfactants Deterg. 16 (5) (2013) 785–794, https://doi.org/10.1007/s11743-013-1449-1.
[64] A.M. Tedeschi, L. Franco, M. Ruzzi, L. Paduano, C. Corvaja, G. D'Errico, Micellar aggregation of alkyltrimethylammonium bromide surfactants studied by electron paramagnetic resonance of an anionic nitroxide, PCCP 5 (19) (2003) 4204–4209, https://doi.org/10.1039/b305324p.
[65] S. Sanjuan, Y. Tran, Stimuli-Responsive Interfaces Using Random Polyampholyte Brushes, Macromolecules 41 (22) (2008) 8721–8728, https://doi.org/10.1021/ma8018798.
[66] S.K. Shah, S.K. Chatterjee, A. Bhattarai, Effect of Methanol on Viscosity of Aqueous Solutions of Cationic Surfactants at 298.15 to 323.15 K, Journal of Chemistry 2016 (2016) 1–5, https://doi.org/10.1155/2016/2176769.
[67] K. Ehtiati, S.Z. Moghaddam, A.E. Daugaard, E. Thormann, How dissociation of carboxylic acid groups in a weak polyelectrolyte brush depend on their distance from the substrate, Langmuir 36 (9) (2020) 2339–2348, https://doi.org/10.1021/acs.langmuir.9b03537.
[68] F. Tiberg, Physical characterization of non-ionic surfactant layers adsorbed at hydrophilic and hydrophobic solid surfaces by time-resolved ellipsometry, Journal of the Chemical Society - Faraday Transactions 92 (4) (1996) 531–538, https://doi.org/10.1039/ft9969200531.
[69] S.B. Velegol, B.D. Fleming, S. Biggs, E.J. Wanless, R.D. Tilton, Counterion effects on hexadecyltrimethylammonium surfactant adsorption and self-assembly on silica, Langmuir 16 (6) (2000) 2548–2556, https://doi.org/10.1021/la9910935.
[70] I.J. Gresham, B.A. Humphreys, J.D. Willott, E.C. Johnson, T.J. Murdoch, G.B. Webber, E.J. Wanless, A.R.J. Nelson, S.W. Prescott, Geometrical confinement modulates the thermoresponse of a poly(*N*-isopropylacrylamide) brush, Macromolecules 54 (5) (2021) 2541–2550, https://doi.org/10.1021/acs.macromol.0c02775.
[71] D. Foreman-Mackey, D.W. Hogg, D. Lang, J. Goodman, emcee : The MCMC Hammer, Publ. Astron. Soc. Pac. 125 (925) (2013) 306–312, https://doi.org/10.1086/670067.
[72] W.D. Vousden, W.M. Farr, I. Mandel, Dynamic temperature selection for parallel tempering in Markov chain Monte Carlo simulations, Mon. Not. R. Astron. Soc. 455 (2) (2016) 1919–1937, https://doi.org/10.1093/mnras/stv2422.
[73] F. Garret-Flaudy, R. Freitag, Unusual thermoprecipitation behavior of poly(*N*,*N*-diethylacrylamide) from aqueous solution in the presence of anionic surfactants, Langmuir 17 (16) (2001) 4711–4716, https://doi.org/10.1021/la001256l.
[74] H. Wang, H. Zhang, S. Yuan, C. Liu, Z. Xu, Molecular dynamics study of the adsorption of anionic surfactant in a nonionic polymer brush, Journal of Molecular Modeling 20 (6) (2014), https://doi.org/10.1007/s00894-014-2267-8.
[75] M.S. Sulatha, U. Natarajan, Molecular dynamics simulations of adsorption of poly(acrylic acid) and poly(methacrylic acid) on dodecyltrimethylammonium chloride micelle in water: effect of charge density, J. Phys. Chem. B 119 (38) (2015) 12526–12539, https://doi.org/10.1021/acs.jpcb.5b04680.
[76] M.C.M. Costa, S.M.C. Silva, F.E. Antunes, Adjusting the low critical solution temperature of poly(*N*-isopropyl acrylamide) solutions by salts, ionic surfactants and solvents: A rheological study, J. Mol. Liq. 210 (2015) 113–118, https://doi.org/10.1016/j.molliq.2015.02.008.
[77] A. Borsos, T. Gil, Interaction of cetyl-trimethylammonium bromide with swollen and collapsed poly(*N*-isopropylacrylamide) nanogel particles, Langmuir 27 (7) (2011) 3461–3467, https://doi.org/10.1021/la200312g.
[78] W. Loh, L.A.C. Teixeira, L.-T. Lee, Isothermal calorimetric investigation of the interaction of poly(*N*-isopropylacrylamide) and ionic surfactants, J. Phys. Chem. B 108 (10) (2004) 3196–3201, https://doi.org/10.1021/jp037190v.
[79] N. Wada, Y. Kajima, Y. Yagi, H. Inomata, S. Saito, Effect of surfactant on the phase transition of *N*-alkylacrylamide gels, Langmuir 9 (1) (1993) 46–49, https://doi.org/10.1021/la00025a013.